ELSEVIER

Inorganica Chimica Acta 229 (1995) 343–354

Inorganica Chimica Acta

# Metal–silicon bonding energetics in organo–Group 4 and organo–f-element complexes. Implications for bonding and reactivity ☆

Wayne A. King, Tobin J. Marks *

*Department of Chemistry, Northwestern University, Evanston, IL 60208-3113, USA*

Received 12 July 1994

**Abstract**

Metal–silicon bond disruption enthalpies have been measured for a series of U, Zr, and Sm metallocene complexes: $Cp_3USi(TMS)_3$, $Cp_2Zr(Cl)Si(TMS)_3$, $Cp_2Zr(Me)Si(TMS)_3$, $Cp_2Zr(TMS)Si(TMS)_3$, $Cp_2Zr(TMS)O\text{-}^tBu$, $Cp'_2SmSiH(TMS)_2$ ($Cp = \eta^5\text{-}C_5H_5$, $Cp' = \eta^5\text{-}Me_5C_5$, TMS = trimethylsilyl). Data were obtained by anaerobic batch-titration solution calorimetry in toluene. Derived metal–ligand bond enthalpies $D(L_nM\text{–}R)$ in kcal mol$^{-1}$ are: $D[Cp_3U\text{–}Si(TMS)_3] = 37(3)$, $D[Cp_2(Cl)Zr\text{–}Si(TMS)_3] = 57(3)$, $D[Cp_2(Me)Zr\text{–}Si(TMS)_3] = 56(5)$, $D[Cp_2(Si(TMS)_3)Zr\text{–}Me] = 66(5)$, $D[Cp_2(O\text{-}^tBu)Zr\text{–}TMS] = 60(5)$, $D[Cp_2(TMS)Zr\text{–}Si(TMS)_3] = 42(11)$, $D[Cp_2(Si(TMS)_3)Zr\text{–}TMS] = 45(7)$, $D[Cp'_2Sm\text{–}SiH(TMS)_2] = 43(5)$. These results show that metal–silicon bond disruption enthalpies involving these electron-deficient metals are substantially smaller than those of the corresponding metal hydride and hydrocarbyl bonds. These data in combination with previously measured metal–ligand bond enthalpies allow thermodynamic analyses of a variety of stoichiometric and catalytic transformations involving metal silyl functionalities. The latter include potential pathways for dehydrogenative silane polymerization, dehydrogenative silane–hydrocarbon coupling, olefin hydrosilylation, and dehydrogenative silane–amine coupling. It is not uncommon for there to be multiple pathways which effect the same catalytic transformation and which contain no steps having major enthalpic impediments.

*Keywords:* Bond enthalpies; Group 4 transition element complexes; Block f-element complexes; Organyl complexes

## 1. Introduction

Early transition metal, lanthanide, and actinide complexes containing metal–silicon bonds display a rich and diverse chemistry [1,2]. This includes a variety of interesting stoichiometric reaction patterns as well as postulated roles in catalytic transformations such as dehydrogenative silane polymerization [1a,3] and olefin hydrosilylation [4]. In addition, there has been considerably theoretical interest in the nature of such metal–metalloid bonds [5]. Recent developments in organometallic chemistry have underscored the unique insights into bonding and reactivity afforded by the acquisition and analysis of metal–ligand bond disruption enthalpies (Eq. (1), (2)) [6,7] and several years ago, we reported thermochemical data on the organoactinide series $Cp_3U\text{–}MPh_3$ ($Cp = \eta^5\text{-}C_5H_5$; M = Si, Ge, Sn) [8].

$$L_nM\text{–}R \longrightarrow L_nM + R^{\cdot} \quad (1)$$

$$D(L_nM\text{–}R) = \Delta H_f^{\circ}(L_nM) + \Delta H_f^{\circ}(R^{\cdot}) - \Delta H_f^{\circ}(L_nM\text{–}R) \quad (2)$$

$L_n$ = ancillary ligands

Although the derived bond enthalpies afford insight into reactions involving U–Si bonds, the data base was clearly limited in the scope of both $L_nM$– and $–SiR_3$ fragments. In the present contribution, we report thermochemical studies of a more extensive series of metal–silyl molecules encompassing Group 4, lanthanide and actinide complexes as well as a broader range of silicon substituents. These data combined with newly revised Si–H bond enthalpy parameters provide a more detailed picture of metal–silyl bonding and reactivity in this part of the Periodic Table.

## 2. Experimental

### 2.1. General considerations

All manipulations of metallocene complexes were carried out under an atmosphere of purified argon

☆ Dedicated to Al Cotton, pioneer, mentor, and friend.

* Corresponding author.


*SSDI* 0020-1693(94)04265-W

using standard high vacuum techniques or in a Vacuum Atmospheres glove-box under prepurified nitrogen. Solvents used were predried and distilled from appropriate drying agents. The toluene used in the calorimetric measurements was stored over Na/K alloy and vacuum transferred immediately prior to use. Iodine was sublimed prior to use. MeI was purified by stirring over Hg and $P_2O_5$, freeze–pump–thaw degassing, and vacuum transferring prior to use. $^1$H NMR spectra were recorded on a Varian XL-400 (400 MHz) or Varian Gemini (300 MHz) spectrometer. Spectra were recorded in $C_6D_6$ and referenced to $SiMe_4$.

### 2.2. Syntheses

Complexes $Cp_2Zr(Cl)Si(TMS)_3$ (**2**) [9], $Cp_2Zr(Me)Si(TMS)_3$ (**3**) [9], $Cp_2Zr(TMS)Si(TMS)_3$ (**4**) [9], $Cp_2Zr(TMS)O$-$^t$Bu (**5**) [10], $Cp'_2SmSiH(TMS)_2$ (**6**) [11], $LiSi(TMS)_3 \cdot 3THF$ (**7**) [12] and $Cp_3UCl$ (**8**) [13] were synthesized and purified according to literature procedures.

#### 2.2.1. $Cp_3USi(TMS)_3$ (1)

A 50 ml flask was charged with **8** (0.651 g, 1.40 mmol) and **7** (0.663 g, 1.41 mmol). Diethyl ether (30 ml) was vacuum transferred onto the solids at −78 °C. The flask was placed under Ar and stirred at −78 °C for 2 h. The brown solution slowly turned deep green. The reaction mixture was then allowed to warm to room temperature over 16 h and stirred for 2 days. The diethyl ether was next removed in vacuo, and the resulting solid was dried under high vacuum for 5 h. Toluene (30 ml) was vacuum transferred at −78 °C onto the olive green solid. The mixture was warmed to room temperature under an Ar atmosphere and supernatant decanted from the remaining solids. The solids were then extracted with toluene until the filtrate was colorless. The toluene was next removed in vacuo. Diethyl ether (15 ml) was vacuum transferred onto the product. A green solution formed. Product solubility decreases considerably in the absence of THF. The green solution was slowly cooled from room temperature to −78 °C and allowed to stand overnight, affording a green microcrystalline solid. The supernatant was then decanted and the product dried in vacuo. Yield 0.715 g (73 %). $^1$H NMR: $\delta$ −3.96 (s, 15H), −6.59 (s, 27H). *Anal.* Calc. for $C_{24}H_{42}Si_4U$: C, 42.3; H, 6.21. Found: C, 42.0; H, 6.23%.

### $^1$H NMR titration experiments

Reactions for calorimetry were monitored via $^1$H NMR titrations to ascertain if each was quantitative and sufficiently rapid for accurate thermochemical measurements. In a Wilmad screw-capped NMR tube fitted with a septum, a known amount of complex was dissolved in $C_6D_6$ and reacted with a solution of the calorimetry reagent, $I_2$ or MeI, in $C_6D_6$ by incremental injection using a Hamilton gas-tight syringe. Each injection was followed by vigorous shaking. For reactions found to be too slow for calorimetry under these conditions, rates were examined by NMR with excess titrant. MeI was used as a $C_6D_6$ solution for reactions requiring stoichiometric quantities and was used neat for reactions requiring excess MeI.

### 2.4. Titration calorimetry

Solution reaction calorimetry was performed in a Tronac model 450 isoperibol calorimeter extensively modified for the study of extremely air- and moisture-sensitive compounds [8,14]. A typical experiment was performed as follows. A metallocene solution of known concentration in toluene was prepared on the day of the experiment as was a toluene solution containing stoichiometrically excess reagent. The reagent and metallocene solution bulbs were then fitted to the calorimeter via solve-seal connections. The calorimeter was evacuated and back-filled several times with Ar. The metallocene solution was then introduced into the calorimeter buret, and the reagent solution was introduced into the reaction dewar under vacuum. The system was then placed under an atmosphere of Ar. Stirring was initiated, and the apparatus was lowered into a constant temperature bath (25.000 ± 0.001 °C) for thermal equilibration. A series of electrical calibration runs was next performed. A series of injections was made using the calibrated, motor driven buret (~12–27 individual injections per run). At the end of the series of titrations, a further set of electrical calibrations was performed. An experimental heat capacity was then derived from the electrical calibration runs. Given the molarity of the reagent and the buret delivery rate, the enthalpy of reaction can be calculated.

## 3. Results

This section begins with a discussion of calorimetric results for complexes **1–6**, and derivations of M–Si bond disruption enthalpies are then presented. In Section 4 these results are considered in terms of patterns in M–Si bonding and the driving forces for a variety of interesting stoichiometric and catalytic transformations.

### 3.1. Iodinolytic calorimetry of complexes 1–6

Complex **1** undergoes clean iodinolysis according to Eq. (3), however the rate is insufficiently rapid for accurate calorimetry in which $I_2$ solutions are titrated

$$Cp_3USi(TMS)_3 + I_2 \longrightarrow Cp_3UI + (TMS)_3SiI \quad (3)$$
**1**

into solutions of excess **1**. However, $^1$H NMR indicates that the titration of **1** solutions into excess $I_2$ also proceeds according to Eq. (3) ($Cp_3UI$ [15] and $(TMS)_3SiI$ [16] were identified from published $^1$H NMR data). In the derivation of $D[Cp_3U\text{–}Si(TMS)_3]$ (Eq. (4)), $D$(I–I) is taken from standard sources [17] and $D(Cp_3U\text{–}I)$ is taken to be equal to the previously determined (absolute)

$$D[Cp_3U\text{–}Si(TMS)_3] = D(Cp_3U\text{–}I) + D[(TMS)_3Si\text{–}I] + \Delta H_{rxn} - D(I\text{–}I) \quad (4)$$

value for $D[(TMSCp)_3U\text{–}I]$ [18]. This is a reasonable approximation since M–halogen bond enthalpies are generally insensitive to ancillary ligation for f elements and early transition metals [8]. An experimental $D[(TMS)_3Si\text{–}I]$ value is not available, and the sensitivity of $D(R_3Si\text{–}X)$ values to TMS substitution [19] suggests $D$(TMS–I) is a poor approximation. Eq. (5) is a more reasonable approximation, utilizing available data for $D[(TMS)_3Si\text{–}H]$ [19a], $D(Me_3Si\text{–}H)$ (=95.1(5) kcal mol$^{-1}$) [20] and $D(Me_3Si\text{–}I)$[1]. Calorimetric and

$$D[(TMS)_3Si\text{–}H]/D(Me_3Si\text{–}H) \approx D[(TMS)_3Si\text{–}I]/D(Me_3Si\text{–}I) \quad (5)$$

derived M–Si bond enthalpy data are collected in Table 1. All uncertainties in $\Delta H_{rxn}$ are reported with 95% confidence limits. All uncertainties for derived $D(L_nM\text{–}R)$ parameters include experimental uncertainties as well as uncertainties in contributing literature parameters. Uncertainties for approximated values used in the derivation of $D(L_nM\text{–}R)$ values are taken to be ±2 kcal mol$^{-1}$.

In a manner similar to that described above, complexes **2–5** were studied by iodinolytic calorimetry (Eqs. (6)–(9)). $^1$H NMR verified that the reactions proceed as shown [16,22]. The result of Eq. (6) is not surprising, since $Cp_2Zr(Cl)I$ is expected to undergo redistribution, in an essentially thermoneutral process, to a statistical mixture of zirconocene halides [22,23].

$$Cp_2Zr(Cl)Si(TMS)_3 + I_2 \longrightarrow \tfrac{1}{3}Cp_2ZrCl_2 + \tfrac{2}{3}Cp_2Zr(Cl)I + \tfrac{1}{3}Cp_2ZrI_2 + (TMS)_3SiI \quad (6)$$

$$Cp_2Zr(Me)Si(TMS)_3 + 2I_2 \longrightarrow Cp_2ZrI_2 + MeI + (TMS)_3SiI \quad (7)$$

$$Cp_2Zr(TMS)Si(TMS)_3 + 2I_2 \longrightarrow Cp_2ZrI_2 + TMSI + (TMS)_3SiI \quad (8)$$

$$Cp_2Zr(TMS)O\text{-}^tBu + I_2 \longrightarrow Cp_2ZrI_2 + TMS(O\text{-}^tBu) \quad (9)$$

$$D[Cp_2(Cl)Zr\text{–}Si(TMS)_3] = D[Cp_2(Cl)Zr\text{–}I] + D[(TMS)_3Si\text{–}I] + \Delta H_{rxn} - D(I\text{–}I) \quad (10)$$

$D[Cp_2(Cl)Zr\text{–}Si(TMS)_3]$ can then be derived (Eq. (10)) using the afore-mentioned value of $D[(TMS)_3Si\text{–}I]$ and $D[Cp_2(Cl)Zr\text{–}I]$, approximated as $D[(Me_5C_5)_2(I)Zr\text{–}I]$ [14b]. This is a reasonable approximation since, as noted above, metal–halogen bond enthalpies are generally rather insensitive to ancillary ligation in this region of the Periodic Table.

The courses of Eqs. (7) and (8) were verified by $^1$H NMR, and the desired Zr–Si bond enthalpies can be obtained via Eqs. (11)–(14). Here, $D$(Zr–Me) in Eq. (12) is approximated by that in $Cp_2ZrMe_2$ (67.2(1.0) kcal mol$^{-1}$) [14b], while $D$(TMS–I) [21] and $D$(Me–I) [24] in all calculations are from standard compilations. The $D[Zr\text{–}Si(TMS)_3]$ value obtained in Eq. (11) is then employed to derive $D$(Zr–TMS) in Eq. (14). Attempts to derive $D$(Zr–TMS) via iodinolysis of $Cp_2Zr(TMS)Cl$ were complicated beyond utility by slow I/Cl exchange between the TMSI product and the zirconocene chloride as well as redistribution of $Cp_2Zr(Cl)I$ (vide supra). The course of Eq. (9) was verified by $^1$H NMR (literature data for TMSO-$^t$Bu [25] and an authentic sample of $Cp_2ZrI_2$). In Eq. (15), $D$[TMS–(O-$^t$Bu)] is taken to be equal to $D$(TMS–OEt) (95(1) kcal mol$^{-1}$) [21] and

$$D[Cp_2(Me)Zr\text{–}SiTMS_3] = 2D[Cp_2(I)Zr\text{–}I] + D(Me\text{–}I) + D[(TMS)_3Si\text{–}I] + \Delta H_{rxn} - 2D(I\text{–}I) - D[Cp_2(Si(TMS)_3)Zr\text{–}Me] \quad (11)$$

$$D[Cp_2(Si(TMS)_3)Zr\text{–}Me] = 2D[Cp_2(I)Zr\text{–}I] + D(Me\text{–}I) + D[(TMS)_3Si\text{–}I] + \Delta H_{rxn} - 2D(I\text{–}I) - D[Cp_2(Me)Zr\text{–}Si(TMS)_3] \quad (12)$$

$$D[Cp_2(Si(TMS)_3)Zr\text{–}TMS] = 2D[Cp_2(I)Zr\text{–}I] + D(TMS\text{–}I) + D(TMS)_3Si\text{–}I - \Delta H_{rxn} - 2D(I\text{–}I) - D[Cp_2(TMS)Zr\text{–}SiTMS_3] \quad (13)$$

$$D[Cp_2(TMS)Zr\text{–}SiTMS_3] = 2D[Cp_2(I)Zr\text{–}I] + D(TMS\text{–}I) + D[(TMS)_3Si\text{–}I] + \Delta H_{rxn} - 2D(I\text{–}I) - D[Cp_2(Si(TMS)_3Zr\text{–}TMS] \quad (14)$$

[1] The enthalpy of formation of $Me_3Si^{\cdot}$ has been recently redetermined [20,21a]. The following values (kcal mol$^{-1}$) for bond enthalpies from Ref. [21b] have been recalculated based on the revised heat of formation of $Me_3Si^{\cdot}$: $D(Me_3Si\text{–}H)$ = 95(1.5), $D(Me_3Si\text{–}Me)$ = 95(1), $D(Me_3Si\text{–}I)$ = 82(1), $D(Me_3Si\text{–}OEt)$ = 120(1), $D(Me_3Si\text{–}NMe_2)$ = 98.

Table 1
Enthalpies of reaction per mole of metal–silyl complexes with various titrants and derived M–Si bond disruption enthalpies in kcal mol$^{-1}$ [a]

| Entry | Compound | Reaction | $\Delta H_{rxn}$ | $D(L_nM-R)$ |
|---|---|---|---|---|
| 1 | $Cp_3USi(TMS)_3$ (**1**) | (3) | −58(1) | 37(3) R = Si(TMS)$_3$ |
| 2 | $Cp_3U-SiPh_3$ | | | 35(4) R = SiPh$_3$ [b]<br>37.3(4.2) R = SiPh$_3$ [c] |
| 3 | $Cp_2Zr(Cl)Si(TMS)_3$ (**2**) | (6) | −56.0(6) | 57(3) R = Si(TMS)$_3$ |
| 4 | $Cp_2Zr(TMS)O\text{-}^tBu$ (**5**) | (9) | −82.5(9) | 58(6) R = TMS [d]<br>60(5) R = TMS [e] |
| 5 | $Cp_2ZrSi(TMS)_3Me$ (**3**) | (7) | −91.9(7) | 56(5) R = Si(TMS)$_3$<br>66(5) R = Me |
| 6 | $Cp_2Zr(TMS)Si(TMS)_3$ (**4**) | (8) | −137(2) | 42(11) R = Si(TMS)$_3$ [f]<br>45(7) R = TMS [g] |
| 7 | $Cp'_2SmSiH(TMS)_2$ (**6**) | (16) | −52(1) | 43(5) R = SiH(TMS)$_2$ |

[a] Quantities in parentheses are 95% confidence limits.
[b] Recalculated from data of Ref. [8], using an improved approximation for $D(Ph_3Si-I)$ (72 kcal mol$^{-1}$), $D(Ph_3Si-I)/D(Ph_3Si-H) \approx D(TMS-I)/D(TMS-H)$, based on $D(Si-H)$ data of Ref. [20].
[c] Ref. [8].
[d] Using $D[Cp_2(TMS)Zr-O\text{-}^tBu] = 105(3)$ kcal mol$^{-1}$ from $D[Cp'_2(C_6F_5O)Zr-O\text{-}^tBu]$ in Ref. [14b] (see discussion in text).
[e] Using $D[Cp_2(TMS)Zr-O\text{-}^tBu] = 103(2)$ kcal mol$^{-1}$ from $D[Cp'_2(CF_3CH_2O)Zr-OCH_2CF_3]$ in Ref. [14b] (see discussion in text).
[f] Calculation based on the measured value of $D(Zr-TMS) = 58(6)$ in entry 4. Large uncertainty reflects propagation of uncertainties in auxiliary data.
[g] Calculation based on the measured value of $D(Cp_2(Cl)Zr-Si(TMS)_3) = 57(3)$ in entry 3.

$$D[Cp_2(O\text{-}^tBu)Zr-TMS] = 2D[Cp_2(I)Zr-I] + D[TMS-(O\text{-}^tBu)] + \Delta H_{rxn} - D(I-I) - D[Cp_2(TMS)Zr-(O\text{-}^tBu)] \quad (15)$$

$D[Cp_2(TMS)Zr-O\text{-}^tBu)]$ to be equal to either $D[Cp'_2(C_6F_5O)Zr-O\text{-}^tBu)]$ (104.6(3.0) kcal mol$^{-1}$ [14b] or $D[Cp'_2(CF_3CH_2O)Zr-OCH_2CF_3]$ (103.2(2.5) kcal mol$^{-1}$) [14b]. Derived Zr–Si bond enthalpies from the calorimetry of Eqs. (6)–(9) are compiled in Table 1.

In contrast to the zirconocene silyls, iodinolysis of **6** does not proceed cleanly, and a mixture of organolanthanide products is formed. In contrast, **6** reacts cleanly and quantitatively with either excess or stoichiometric MeI according to Eq. (16). The products $MeSiHTMS_2$ [26] and $(Cp_2SmI)_x$ [14a] were identified by $^1$H NMR. The quantity $D[(TMS)_2HSi-Me]$ required in Eq. (17) was reasonably estimated via Eq. (18), where $D[(TMS)_2MeSi-H]$ is estimated to be 83 kcal mol$^{-1}$ either from linear correlations between

$$Cp'_2SmSiH(TMS)_2 + MeI \longrightarrow \underset{(6)}{} \frac{1}{x}(Cp'_2SmI)_x + MeSiH(TMS)_2 \quad (16)$$

$$D(Cp'_2Sm-SiH(TMS)_2] = D(Cp'_2Sm-I) + D[(TMS)_2HSi-Me] + \Delta H_{rxn} - D(Me-I) \quad (17)$$

$D(Si-H)$ and $n$ for $(TMS)_nMe_{3-n}SiH$ compounds [2] or

$$D[(TMS)_2HSi-Me]/D(TMS-Me) \approx D[(TMS)_2MeSi-H]/D(TMS-H) \quad (18)$$

from $D(Si-H)/\nu(Si-H)$ correlations [19b]. $D(Cp'_2Sm-I)$ is taken from previous work [8] and $D(Me_3Si-Me)$ and $D(Me_3Si-H)$ from recent recalculations [20,21]. The resulting $D(Sm-Si)$ value is given in Table 1.

## 4. Discussion

### 4.1. Bonding trends

The present results expand considerably what is known about metal–silyl bonding energetics for Group 4, actinides, and lanthanides. One generalization is readily apparent from the comparative data in Table 2 – the metal–silyl bond enthalpies are rather modest. In most cases, metal–silyl bonds are ~10 kcal mol$^{-1}$ weaker than the corresponding metal–Me bonds. In most cases, differences in M–R bonding energetics between R = $SiPh_3$, $-SiMe_3$ and $-Si(TMS)_3$ are insignificant for constant M. It also appears from Tables 1 and 2 that ancillary ligand effects on $D(M-Si)$ are generally small, as can be seen in Table 1 entries 3, 4 and 5. The only exception may be $Cp_2Zr(TMS)Si(TMS)_3$, where steric congestion is a likely factor (entry 6).

The relative weakness of the present Group 4/4f/5f metal–silyl bonds can be rationalized along two com-

[2] A plot of $D(Si-H)$ vs. $n$ yields an approximately linear relationship ($R = 0.951$).

Table 2
Comparison of metal–silyl bond enthalpies with those of other metal–ligand $\sigma$-bonds

| Compound | $D$(M–M′)/$D$(M–R) | Ref. |
|---|---|---|
| $Cp'_2(C_6F_5O)Zr$–$OC_6F_5$ | 105(3) | [14b] |
| $Cp'_2(CF_3CH_2O)Zr$–$OCH_2CF_3$ | 103(2) | [14b] |
| $Cp'_2(I)Zr$–I | 80.4(0.5) | [14b] |
| $Cp'_2(H)Zr$–H | 78(1) | [14b] |
| $Cp'_2(Ph)Zr$–Ph | 73.1(3.5) | [14b] |
| $Cp'_2(Me)Zr$–Me | 67(1) | [14b] |
| $Cp_2(Me)Zr$–Me | 67(1) | [23] |
| $Cp_2(Cl)Zr$–$Si(TMS)_3$ | 57(3) | this study |
| $Cp_2(O^tBu)Zr$–$SiMe_3$ | 59(5) | this study |
| $Cp_2(Me)Zr$–$Si(TMS)_3$ | 56(5) | this study |
| $Cp_2[(TMS)_3Si]Zr$–$SiMe_3$ | 45(7) | this study |
| $Cp_2(TMS)Zr$–$Si(TMS)_3$ | 42(11) | this study |
| $(TMSCp)_3U$–I | 62.4(0.4) | [18] |
| $(TMSCp)_3U$–H | 60(1) | [27] |
| $(TMSCp)_3U$–Me | 45(1) | [18] |
| $(TMSCp)_3U$–$^n$Bu | 29(2) | [18] |
| $Cp_3U$–$SiPh_3$ | 35(4) | [8] |
| $Cp_3U$–$Si(TMS)_3$ | 37(3) | this study |
| $Cp_3U$–$GePh_3$ | 38.9(4.5) | [8] |
| $Cp'_2Sm$–O$^t$Bu | 81(1) | [14a] |
| $Cp'_2Sm$–I | 69(2) | [14a] |
| $Cp'_2Sm$–H | 52(2) | [14a] |
| $Cp'_2Sm$–$NMe_2$ | 48(2) | [14a] |
| $Cp'_2Sm$–$CHTMS_2$ | 47(1) | [14a] |
| $Cp'_2Sm$–$SiH(TMS)_2$ | 43(5) | this study |

plementary lines of argument. As pointed out previously [14b,28], Pauling-like electronegativity considerations can be used to understand gross trends in metal–ligand bonding. Thus, electropositive metals as in the present case will tend to form the strongest bonds to electronegative ligands such as alkoxide, halide, while less electronegative ligands such as silyl ($\chi$(Si) = 1.90) [29] should form weaker bonds than alkyl ($\chi(CH_3) = 2.30$) [29] and hydride ($\chi$(H) = 2.20) [29]. In a complementary molecular orbital picture, attractive/$\pi$-donor interactions/overlap between filled $-CH_3$ orbitals of $\pi$ symmetry and empty ($d^0$) metal orbitals are expected to be much stronger than analogous interactions involving silyl ligands. In contrast, silyl ligands have low-lying $\pi$ symmetry acceptor orbitals, and backdonation from electron-rich later transition metals is expected to be stronger than for $-CH_3$ ligands [5a–c,e]. Ab initio calculations at the MP2/III/MP2/III (RHF/III/MP2/III) level [5a] indicate that $D(Zr–CH_3) - D(Zr–SiH_3) = 14.3(11.7)$ kcal mol$^{-1}$ in $Cl_2Zr(EH_3)H$ complexes (E = C, Si), in good agreement with the present results (Table 2), especially considering the differing steric environments. The same level of ab initio calculations indicate that $D(Rh–CH_3) - D(Rh–SiH_3) = -20.4(-22.3)$ kcal mol$^{-1}$ in $(Ph_3P)_2(H)Rh(Cl)(EH_3)$ complexes [5a].

Striking similarities in $(Cp/TMSCp)_3U$–R/X, $Cp'_2Zr$–$R_2/X_2$ and $Cp'_2Ln$–R/X metal–ligand bonding energetics have been noted previously [14a,28]. Fig. 1 illustrates where $D$(M–Si) values fit into the respective scales of metal–ligand enthalpies and also that $D$(M–Si) parameters conform to the afore-mentioned interperiod transferability trends. The relationships are generally rather linear, with the associated character of certain samarium complexes ($(Cp'_2SmX)_x$, X = H, I, OR) [14a] and possible cases of severe non-bonded repulsions likely sources of scatter.

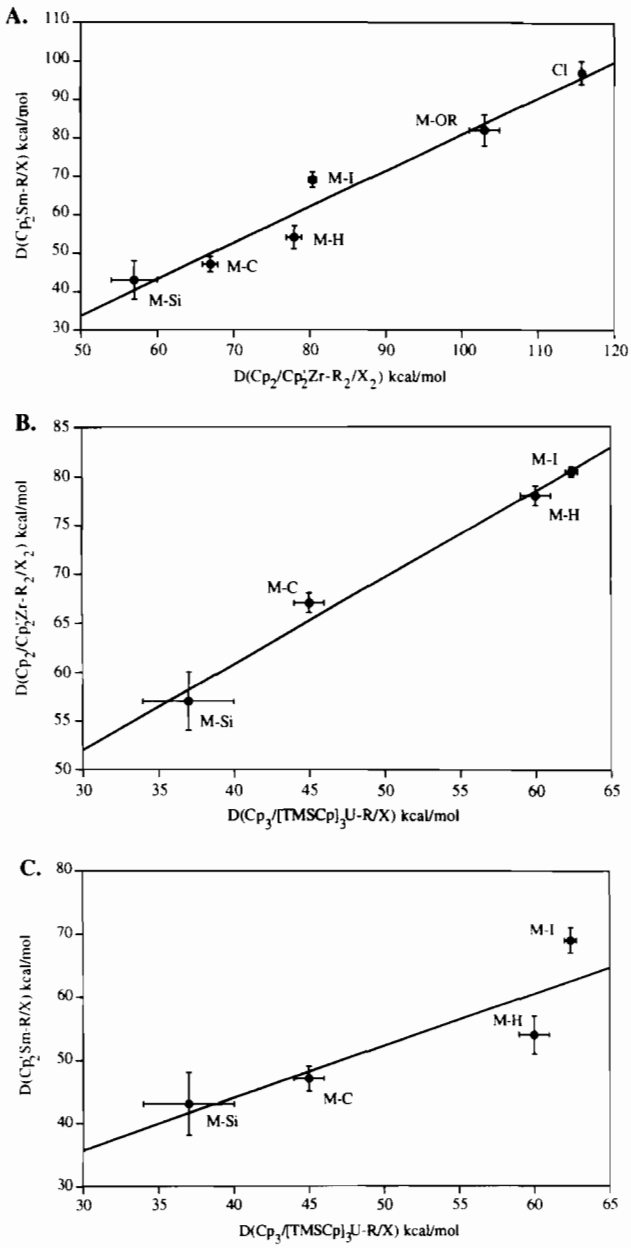


Fig. 1. (A) Comparison of $D(C'_2Sm$-R/X) data to the corresponding $D(Cp_2/Cp'_2Zr–R_2/X_2)$ data. The line is a least-squares fit to the data points ($R$ = 0.977). (B) Comparison of $D(Cp_2/Cp'_2Zr–R_2/X_2)$ data to the corresponding $D$[(Cp/TMSCp)$_3$U–R/X] data. The line is a least-squares fit to the data ($R$ = 0.993). (C) Comparison of $D(Cp'_2Sm$–R/X) data to the corresponding $D$[(Cp/TMSCp)$_3$U–R/X] data. The line is a least-squares fit to the data ($R$ = 0.986).

### 4.2. Thermochemistry of known and hypothetical M–Si-centered transformations

The bond enthalpy data of Tables 1 and 2 combined with parameters extrapolated from the afore-mentioned $L_nM-X/R - L'_nM'-X/R$ trends [14a,28], and necessary ancillary data [17,19–21] allows an approximate thermochemical analysis of a variety of stoichiometric and catalytic transformations involving silyl functionalities. Of particular interest also will be comparisons involving differing $L_nM-$ frameworks.

The present zirconocene data allow an examination of reductive elimination/coupling processes which may be important in certain Group 4-centered catalytic cycles which form Si–C or Si–Si bonds [3,4]. Taking $D(\text{Zr–Si}) \approx 58$ kcal mol$^{-1}$ (cf. entries 3,4,5 in Table 1) and $D(\text{Si–Si}) \approx 79(3)$ kcal mol$^{-1}$ [21a] leads to the conclusion that such processes will be rather endothermic (Eqs. (19)–(21)). Even in the most optimistic case where there appear to be severe non-bonded repulsions (Table 1, entry 6) [3], reductive coupling

$$Cp_2Zr(SiR_3)(H) \longrightarrow Cp_2Zr + R_3Si{-}H \quad (19)$$

$\Delta H_{calc} \approx +41$ kcal mol$^{-1}$

$$Cp_2Zr(SiR_3)(CH_3) \longrightarrow Cp_2Zr + R_3Si{-}CH_3 \quad (20)$$

$\Delta H_{calc} \approx +31$ kcal mol$^{-1}$

$$Cp_2Zr(SiR_3)(SiR_3) \longrightarrow Cp_2Zr + R_3Si{-}SiR_3 \quad (21)$$

$\Delta H_{calc} \approx +37$ kcal mol$^{-1}$

$$Cp_2Zr(SiR_3)(SiR'_3) \longrightarrow Cp_2Zr + R_3Si{-}SiR'_3 \quad (22)$$

$\Delta H_{calc} \approx +8$ kcal mol$^{-1}$

is predicted to be endothermic (Eq. (22)), although entropic contributions ($T\Delta S \approx +6$ to $+12$ kcal mol$^{-1}$) [30] may now render it exergonic. Complexation of $Cp_2Zr$ with olefin present in certain catalytic cycles, might impart additional enthalpic driving force in Eqs. (19)–(22).

Early transition metal silyl complexes have been reported to effect C–H bond scission in (aromatic) hydrocarbons [31], and the microscopic reverse represents a viable synthetic pathway for forming metal–silyl bonds [1,2]. As can be seen in Eqs. (23)–(28), such processes are generally near thermoneutrality and

$$\text{Zr–Si} + \text{Ph–H} \longrightarrow \text{Zr–Ph} + \text{Si–H} \quad (23)$$

$\Delta H_{calc} \approx +1.0$ kcal mol$^{-1}$

$$\text{Sm–Si} + \text{Ph–H} \longrightarrow \text{Sm–Ph} + \text{Si–H} \quad (24)$$

$\Delta H_{calc} \approx +14$ kcal mol$^{-1}$

$$\text{U–Si} + \text{Ph–H} \longrightarrow \text{U–Ph} + \text{Si–H} \quad (25)$$

$\Delta H_{calc} \approx 0$ kcal mol$^{-1}$

$$\text{Zr–Si} + \text{Me–H} \longrightarrow \text{Zr–Me} + \text{Si–H} \quad (26)$$

$\Delta H_{calc} \approx -1.0$ kcal mol$^{-1}$

$$\text{Sm–Si} + \text{Me–H} \longrightarrow \text{Sm–Me} + \text{Si–H} \quad (27)$$

$\Delta H_{calc} \approx +5.0$ kcal mol$^{-1}$

$$\text{U–Si} + \text{Me–H} \longrightarrow \text{U–Me} + \text{Si–H} \quad (28)$$

$\Delta H_{calc} \approx 0$ kcal mol$^{-1}$

could, in principle, be driven in either direction by appropriate choice of reaction conditions. The only conspicous exception is the estimate of Eq. (24), which appears to reflect either an unrealistic estimated $D$(Sm–Ph) value or an anomalously strong Sm–SiH(TMS)$_2$ bond (Table 1). These results are somewhat more exothermic than implied by the organouranium result reported previously [8], owing to the recently revised (redetermined) value for $D(Me_3Si–H)$ [20]. Berry has measured, via equilibration techniques, the thermodynamics of arene addition to $Cp_2Ta(PMe_3)SiR_3$ complexes to yield $Cp_2Ta(PMe_3)Ar$ products (analogous to Eqs. (23)–(25)) [31c]. He concludes that $D(\text{Ta–Ph}) - D(\text{Ta–Si}) = 5.4–7.9$ kcal mol$^{-1}$. That this difference is somewhat smaller than the present results (14–17 kcal mol$^{-1}$; Table 2) appears to reflect the afore-mentioned capacity of later metals ($d^2$ versus $d^0$) to backbond to silyl $\pi$ acceptor orbitals [5].

A priori, hydrocarbon activation could take a pathway of polarization opposite to that of Eqs. (23)–(28) in which the metal-bound silicon is transferred to the hydrocarbyl residue. As illustrated in Eqs. (29)–(31) [4], such processes are estimated to be more exothermic than Eqs. (23)–(28).

$$\text{Zr–Si} + \text{Ph–H} \longrightarrow \text{Zr–H} + \text{Si–Ph} \quad (29)$$

$\Delta H_{calc} \approx -13$ kcal mol$^{-1}$

[3] In this case, it may be unrealistic to use the $D$(Si–Si) of $Me_3SiSiMe_3$ for such bulky substituents.

[4] $D(Me_3Si–Ph)$ is estimated from average ($\bar{D}$) values [32] as $D(Me_3Si–Ph) \approx [\bar{D}(SiPh_4)/\bar{D}(SiMe_4)]D(Me_3Si–Me)$. This yields 104 kcal mol$^{-1}$.

$$Sm\text{–}Si + Ph\text{–}H \longrightarrow Sm\text{–}H + Si\text{–}Ph \quad (30)$$

$\Delta H_{calc} \approx -2$ kcal mol$^{-1}$

$$U\text{–}Si + Ph\text{–}H \longrightarrow U\text{–}H + Si\text{–}Ph \quad (31)$$

$\Delta H_{calc} \approx -17$ kcal mol$^{-1}$

$$Zr\text{–}Si + Me\text{–}H \longrightarrow Zr\text{–}H + Si\text{–}Me \quad (32)$$

$\Delta H_{calc} \approx -11$ kcal mol$^{-1}$

$$Sm\text{–}Si + Me\text{–}H \longrightarrow Sm\text{–}H + Si\text{–}Me \quad (33)$$

$\Delta H_{calc} \approx 0$ kcal mol$^{-1}$

$$U\text{–}Si + Me\text{–}H \longrightarrow U\text{–}H + Si\text{–}Me \quad (34)$$

$\Delta H_{calc} \approx -15$ kcal mol$^{-1}$

Closely related to Eqs. (23)–(31) are processes by which metal-bound hydrocarbyl groups are transferred to silicon (Eqs. (35)–(40)). This reaction pattern is proposed to be a key step in organolanthanide-catalyzed olefin hydrosilylation (vide infra) [4h,i], and the present analysis argues that it is generally exothermic for aryl

$$Zr\text{–}Ph + Si\text{–}H \longrightarrow Zr\text{–}H + Si\text{–}Ph \quad (35)$$

$\Delta H_{calc} \approx -14$ kcal mol$^{-1}$

$$Sm\text{–}Ph + Si\text{–}H \longrightarrow Sm\text{–}H + Si\text{–}Ph \quad (36)$$

$\Delta H_{calc} \approx -16$ kcal mol$^{-1}$

$$U\text{–}Ph + Si\text{–}H \longrightarrow U\text{–}H + Si\text{–}Ph \quad (37)$$

$\Delta H_{calc} \approx -17$ kcal mol$^{-1}$

$$Zr\text{–}Me + Si\text{–}H \longrightarrow Zr\text{–}H + Si\text{–}Me \quad (38)$$

$\Delta H_{calc} \approx -11$ kcal mol$^{-1}$

$$Sm\text{–}Me + Si\text{–}H \longrightarrow Sm\text{–}H + Si\text{–}Me \quad (39)$$

$\Delta H_{calc} \approx -5$ kcal mol$^{-1}$

$$U\text{–}Me + Si\text{–}H \longrightarrow U\text{–}H + Si\text{–}Me \quad (40)$$

$\Delta H_{calc} \approx -15$ kcal mol$^{-1}$

and alkyl functionalities. Summarizing, in regard to the silanolysis of organo–Group 4 and f-element hydrocarbyls, the comparative thermodynamics of the various competing pathways are as shown below. It can be seen below that the processes which create C–Si bonds are generally more favorable.

$$M\text{—}Me + Si\text{—}H \longrightarrow \begin{cases} M\text{—}H + Si\text{—}Me & \Delta H_{calc} \approx -5 \text{ to } -15 \text{ kcal mol}^{-1} \\ M\text{—}Si + H\text{—}Me & \Delta H_{calc} \approx +1 \text{ to } -5 \text{ kcal mol}^{-1} \end{cases}$$

$$M\text{—}Ph + Si\text{—}H \longrightarrow \begin{cases} M\text{—}H + Si\text{—}Ph & \Delta H_{calc} \approx -14 \text{ to } -17 \text{ kcal mol}^{-1} \\ M\text{—}Si + H\text{—}Ph & \Delta H_{calc} \approx 0 \text{ to } -14 \text{ kcal mol}^{-1} \end{cases}$$

Hydrogenolysis of metal–silyl linkages and its microscopic reverse are potentially important reactions which have been invoked in metal-catalyzed silane transformations [1a,2c]. The present data along with the revised (higher) value of $D$(Si–H) argue that such processes can be rather exothermic (Eqs. (41)–(43)). Similarly, Eqs. (44)–(46) describe an analogous Si–Si bond-forming reaction that is believed to be a key

$$Zr\text{–}Si + H_2 \longrightarrow Zr\text{–}H + H\text{–}Si \quad (41)$$

$\Delta H_{calc} \approx -11$ kcal mol$^{-1}$

$$Sm\text{–}Si + H_2 \longrightarrow Sm\text{–}H + H\text{–}Si \quad (42)$$

$\Delta H_{calc} \approx -0$ kcal mol$^{-1}$

$$U\text{–}Si + H_2 \longrightarrow U\text{–}H + H\text{–}Si \quad (43)$$

$\Delta H_{calc} \approx -15$ kcal mol$^{-1}$

step in early transition metal/f-element-catalyzed dehydrogenative silane polymerization. It can be seen that such processes are usually exothermic.

$$Zr\text{–}Si + Si\text{–}H \longrightarrow Zr\text{–}H + Si\text{–}Si \quad (44)$$

$\Delta H_{calc} \approx -4$ kcal mol$^{-1}$

$$Sm\text{–}Si + Si\text{–}H \longrightarrow Sm\text{–}H + Si\text{–}Si \quad (45)$$

$\Delta H_{calc} \approx +7$ kcal mol$^{-1}$

$$U\text{–}Si + Si\text{–}H \longrightarrow U\text{–}H + Si\text{–}Si \quad (46)$$

$\Delta H_{calc} \approx -8$ kcal mol$^{-1}$

Olefin insertion into metal–silyl bonds is a known transformation [1,2d] and one that is likely important for hydrosilylation processes catalyzed by some metal complexes [33]. In regard to the metal centers under consideration, Eqs. (47)–(49) show that the process is decidedly exothermic.

$$Zr\text{–}Si + \| \longrightarrow \overset{/}{Zr}\overset{\backslash}{\quad}Si \quad (47)$$

$\Delta H_{calc} \approx -23$ kcal mol$^{-1}$

$$Sm\text{–}Si + \| \longrightarrow \overset{\frown}{Sm}\quad\overset{\frown}{Si} \qquad (48)$$

$\Delta H_{calc} \approx -24$ kcal mol$^{-1}$

$$U\text{–}Si + \| \longrightarrow \overset{\frown}{U}\quad\overset{\frown}{Si} \qquad (49)$$

$\Delta H_{calc} \approx -20$ kcal mol$^{-1}$

The present bond enthalpy data also allow an analysis of various metal–silyl reaction pathways involving heteroatom reagents, which are relevant to catalyzed silane–heteroatom dehydrocoupling processes [34]. We illustrate this here with the amine/amido functionality being $Me_2NH/Me_2N$–. It can be seen in Eqs. (50)–(55), that although protonolysis pathways are estimated to

$$Zr\text{–}Si + H\text{–}NMe_2 \longrightarrow Zr\text{–}NMe_2 + Si\text{–}H \qquad (50)$$

$\Delta H_{calc} \approx -22$ kcal mol$^{-1}$

$$Sm\text{–}Si + H\text{–}NMe_2 \longrightarrow Sm\text{–}NMe_2 + Si\text{–}H \qquad (51)$$

$\Delta H_{calc} \approx -8$ kcal mol$^{-1}$

$$U\text{–}Si + H\text{–}NMe_2 \longrightarrow U\text{–}NMe_2 + Si\text{–}H \qquad (52)$$

$\Delta H_{calc} \approx -10$ kcal mol$^{-1}$

be exothermic, those forming Si–N bonds are more so (Eqs. (53)–(55)).

$$Zr\text{–}Si + H\text{–}NMe_2 \longrightarrow Zr\text{–}H + Me_2N\text{–}Si \qquad (53)$$

$\Delta H_{calc} \approx -26$ kcal mol$^{-1}$

$$Sm\text{–}Si + H\text{–}NMe_2 \longrightarrow Sm\text{–}H + Me_2N\text{–}Si \qquad (54)$$

$\Delta H_{calc} \approx -15$ kcal mol$^{-1}$

$$U\text{–}Si + H\text{–}NMe_2 \longrightarrow U\text{–}H + Me_2N\text{–}Si \qquad (55)$$

$\Delta H_{calc} \approx -30$ kcal mol$^{-1}$

Organo–group 4 and organo–f-element complexes catalyze a diverse range of transformations involving silanes and possibly metal silyls. It is instructive to examine the thermodynamic contraints under which various possible cycles must operate. We begin with dehydrogenative silane polymerization (Eq. (56)) [1a,3]. Although the precise thermodynamics of this process are not readily estimated with the information currently in hand, data are available to accurately calculate $\Delta H$ for model dehydrodimerizations (Eq. (57)). For R = Me, revised $D$(Si–H) parameters [20,21]

$$n RSiH_3 \longrightarrow H\text{–}\left(\begin{matrix} R \\ Si \\ H \end{matrix}\right)_n\text{–}H + (n-1)H_2 \qquad (56)$$

$$2R_3Si\text{–}H \longrightarrow R_3Si\text{–}SiR_3 + H_2 \qquad (57)$$

$\Delta H_{calc} \approx +7$ kcal mol$^{-1}$ (R = Me)

indicate that this reaction is not as exothermic as previously thought, and that loss/removal of $H_2$ must be a major driving force. In regard to the propagation mechanism, several lines of evidence argue against oxidative addition/reductive elimination sequences and in favor of four-center heterolytic, '$\sigma$-bond metathesis' processes. This includes model reactions [1a,3b], the efficacy of organolanthanide catalysts [3e] and the marked calculated endothermicity of the reductive coupling processes depicted in Eqs. (19)–(21). Scheme 1 illustrates estimated enthalpy changes for cycles involving both R = Me and R = H substrates. Parameters for the latter silane species are taken from recent tabulations [20] while $D$(M–Si) values are those in Table 1. It can be seen that for all three metal centers, step i in the catalytic cycle is the most endothermic, while the Si–Si coupling step is also estimated to be exothermic except in the case of the organosamarium catalyst (reflecting the relative weakness of an Sm–H bond versus what may be an anomalous Sm–Si bond — vide supra). It can also be seen in Scheme 1 that the effect of the silicon substituents on the thermodynamics of the various steps is not large. That the sums of $\Delta H_{calc}$ for steps i and ii are in excellent agreement with $\Delta H$ for Eq. (57) serves as an internal check on the self-consistency of the ancillary data and the calorimetric results.

The dehydrogenative coupling of silanes and hydrocarbons to yield alkylsilanes would appear to be an attractive alternative, *direct* route to such molecules (e.g. Eq. (58)) [5]. Schemes 2–4 explore several me-

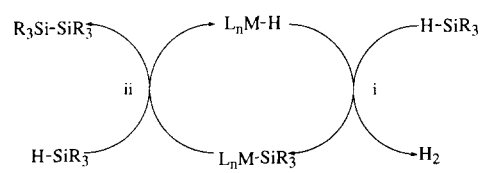


| R = Me, $\Delta H_{calcd}$, kcal/mol | R = Me, $\Delta H_{calcd}$, kcal/mol |
|---|---|
| Zr ≈ -4 | Zr ≈ +11 |
| Sm ≈ +7 | Sm ≈ 0 |
| U ≈ -8 | U ≈ +15 |
| **R = H, $\Delta H_{calcd}$, kcal/mol** | **R = H, $\Delta H_{calcd}$, kcal/mol** |
| Zr ≈ -6 | Zr ≈ +10 |
| Sm ≈ +6 | Sm ≈ -2 |
| U ≈ -8 | U ≈ +12 |

Scheme 1.

[5] Traditional routes to alkyl silanes employ silyl halides and metallic reagents or silanes and unsaturated organics [35a,b]. Aryl silanes have been prepared directly from silanes and arenes at very high temperatures, see Ref. [35a], p. 26.

$$Me_3Si{-}H + CH_4 \longrightarrow Me_3Si{-}CH_3 + H_2 \qquad (58)$$

$\Delta H_{calc} \approx 0$

chanistically distinct cycles for the dehydrogenative fusion of methane and trimethylsilane. Scheme 2 produces an M–Si functionality (cf. Eqs. (41)–(43)) which is then transferred to the hydrocarbon in a C–H activating process (Eqs. (29)–(34)). There is ample precedent for the reverse of endothermic step i [1a,2c]. Furthermore, the sums of $\Delta H_{calc}$ for steps i and ii are in generally good agreement with Eq. (58). Scheme 3 couples metal silyl C–H activation (for which there is precedent for arenes) [31] with alkyl transfer from metal to silane (for which there is precedent [4h,i] and the reverse of silane hydrogenolysis (for which there is precedent) [1a,2c]. The $\Delta H_{calc}$ sums are in excellent agreement with Eq. (58) for all three metals. Finally, Scheme 4 couples the microscopic reverse of metal hydrocarbyl hydrogenolysis (for which there is precedent in both directions) [14,36] with alkyl transfer to a silane (for which there is precedent [1a,2c]). Step i is estimated to be endothermic (but in some cases is known to be kinetically accessible [36]) while step ii is calculated to be exothermic. These results indicate that there are multiple potential pathways by which an electrophilic metal center could mediate alkane coupling with silanes.

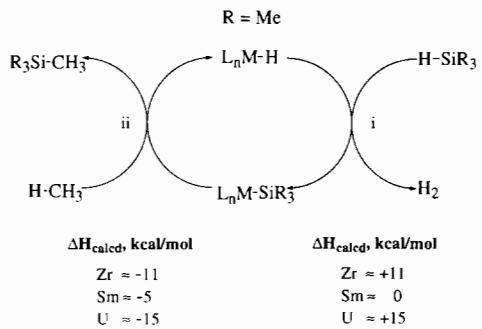


Scheme 2.

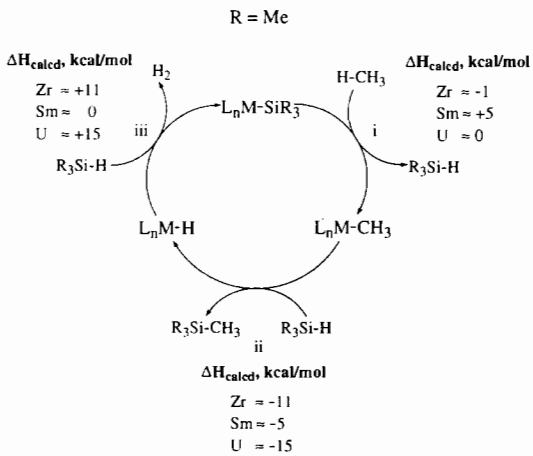


Scheme 3.

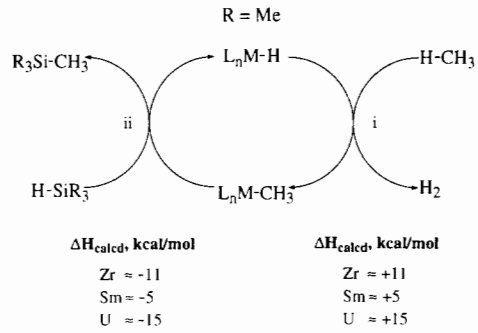


Scheme 4.

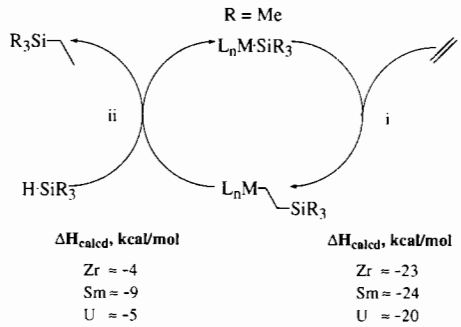


Scheme 5.

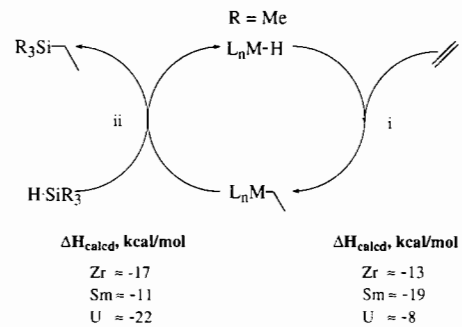


Scheme 6.

Organo–Group 4 and –lanthanide complexes are active homogeneous olefin hydrosilylation catalysts [4], and as pointed at previously [8], there are two distinct catalytic cycles which, in principle, can effect this transformation. Schemes 5 and 6 summarize the pathways and the relevant enthalpic changes for the simple case of ethylene and trimethylsilane. Scheme 5 is a metal silyl based cycle which invokes olefin insertion into a metal–silyl bond (Eqs. (47)–(49); for which, as noted above, there is precedent), followed by what is essentially 'protonolysis' of the metal hydrocarbyl to yield silylated alkane and metal silyl (the microscopic reverse of Eqs. (26)–(28)). The second step is considerably less exothermic. Using tabulated thermochemical data [20,21], we estimate that $\Delta H$ for $Et_3SiH + \| \rightarrow Et_4Si$ is $\sim -29$ kcal $mol^{-1}$, in reasonable agreement with the individual $\Delta H$ sums steps i and ii in Scheme 5. Scheme 6 is a metal hydride-based cycle which is formally analogous to the catalytic hydrogenation of olefins by these metals

[36a–c,37]. Exothermic insertion of olefin into the metal hydride bond [38] (step i) is followed by silanolysis (rather than hydrogenolysis) of the resulting metal hydrocarbyl (step ii). Transfer of the hydrocarbyl group to silicon then yields the product. Again the $\Delta H$ sums for steps i and ii approximate the estimated $\Delta H$ of the overall reaction.

Comparing Schemes 5 and 6, it can be seen that the former requires an initially exothermic but likely sluggish (sterically impeded) [2d] olefin insertion followed by an M–C cleavage which has little driving force and which formally polarizes groups in an unusual manner for a silane (**A** versus **B**) [39]. In contrast, Scheme 6 invokes an exothermic and kinetically facile olefin

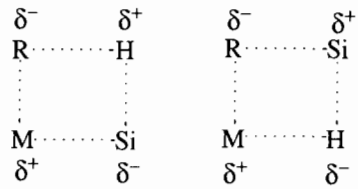

**A** **B**

insertion into a metal hydride bond [37,38] followed by an exothermic (but probably slower) hydrocarbyl transfer via more conventional transition state **B**. In mechanistic studies to be discussed fully elsewhere [4h,i], we find that the organolanthanide-catalyzed hydrosilylation of styrenic olefins by $PhSiH_3$ proceeds via a pathway suggestive of Scheme 6, with the rate law exhibiting zero-order behavior in olefin and first-order behavior in silane – a not unexpected kinetic scenario.

Liu and Harrod have reported that $Cp_2TiMe_2$ is an efficient catalyst for the dehydrogenative coupling of aryl silanes with $NH_3$ to yield low molecular weight disilazanes (Eq. (59)) [34]. Two possible catalytic

$$\text{Si–H} + \text{H–N} \longrightarrow \text{Si–N} + \text{H}_2 \qquad (59)$$

$\Delta H_{calc} \approx -15$ kcal mol$^{-1}$

cycles for this process are analyzed in Schemes 7 and 8. The former couples the moderately endothermic reverse of metal silyl hydrogenolysis (Eqs. (41)–(43) with exothermic transfer of silyl group from metal to

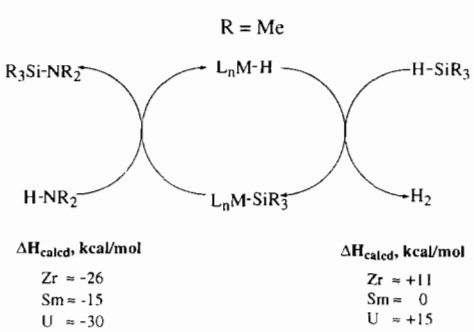


Scheme 7.

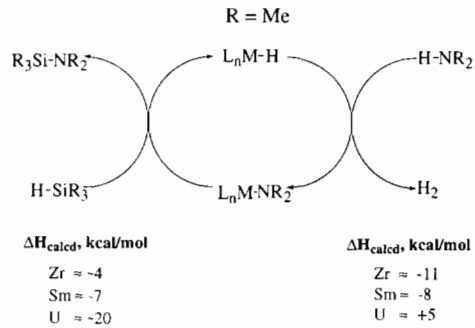


Scheme 8.

nitrogen (Eqs. (53)–(55)). The enthalpy of the latter transformation reflects the prodigious strength of silicon–heteroatom bonds [20,21]. Scheme 8 couples amide-forming metal hydride protonolysis [14] with amide-to-silicon transfer. In most cases, both steps are estimated to be exothermic.

## 5. Conclusions

The results of this study considerably expand the knowledge base concerning metal–silyl bonding energetics involving Group 4 and f metals. The picture is one of relatively weak bonds. Nevertheless, for thermodynamic reasons that are evident in the analyses of reactant → product bond enthalpy changes, these linkages can participate in a wide range of stoichiometric and catalytic processes. Particularly interesting is the observation that hydrocarbon/olefin/silane catalytic cycles can have a multiplicity of multi-step manifolds which effect the same transformation and the steps of which have no major enthalpic barriers.

## Acknowledgements

We thank NSF for generous support of this research under Grant CHE9104112. We thank Professor D.H. Berry for information in advance of publication.

## References

[1] (a) T.D. Tiley, *Acc. Chem. Res., 26* (1993) 22–29, and refs. therein; (b) *Comments Inorg. Chem., 10* (1) (1990) 37–51, and refs. therein; (c) in S. Patai and Z. Rappoport (eds.), *The Chemistry of Organic Silicon Compounds,* Wiley, Chichester, UK, 1989, Ch. 24, and refs. therein.

[2] (a) B.K. Campion, R.H. Heyn and T.D. Tilley, *Organometallics, 12* (1993) 2584–2590; (b) N.S. Radu, T.D. Tilley and A.L. Rheingold, *J. Am. Chem. Soc., 114* (1992) 8293–8295; (c) H.-G. Woo, W.P. Freeman and T.D. Tilley, *Organometallics, 11* (1992) 2198–2205; (d) K. Kreutzer, R.A. Fisher, W.M. Davis, E. Spaltenstein and S.L. Buchwald, *Organometallics, 10* (1991) 4301–4335, and refs. therein; (e) J. Arnold, M.P. Engeles, F.H.

Eisener, R.H. Heyn and T.D. Tilley, *Organometallics, 8* (1989) 2284–2286.

[3] (a) J.Y. Corey, J.L. Huhmann and X.-H. Zhu, *Organometallics, 12* (1993) 1121–1130, and refs. therein; (b) H.-G. Woo, J.F. Walzer and T.D. Tilley, *J. Am. Chem. Soc., 114* (1992) 7047–7055; (c) J.F. Harrod, in R.M. Lain (ed.), *Inorganic and Organometallic Polymers with Speical Properties,* Kluwer, Amsterdam, Netherlands, 1991, Ch. 14, and refs. therein; (d) T. Kobayashi, T. Sakakura, T. Hayashi, M. Yumura and M. Tanaka, *Chem. Lett.,* (1992) 1157–1160; (e) C.M. Forsyth, S.P. Nolan and T.J. Marks, *Organometallics, 10* (1991) 2543–2545; (f) P.L. Watson and F.N. Tebbe, *US Patent No. 4 965 386* (1990).

[4] (a) G.A. Molander and M. Julius, *J. Org. Chem., 57* (1992) 6347–6351; (b) M.R. Kesti and R.M. Waymouth, *Organometallics, 11* (1992) 1095–1103; (c) T. Takahashi, M. Hasegawa, N. Suzuki, M. Saburi, C.J. Rousset, P.E. Fanwick and E. Negishi, *J. Am. Chem. Soc., 113* (1991) 8564–8566; (d) T. Sakakura, H.-J. Lautenschlager and M. Tanaka, *J. Chem. Soc., Chem. Commun.,* (1991) 40–41; (e) I.P. Beletskaya, A.Z. Voakoboinikov, I.N. Parshina and G.K.-I. Magomedov, *Izv. Akad. Nauk. SSSR,* (1990) 693–694; (f) T.J. Marks, *1st Int. Conf. f-Elements, Leuven, Belgium, Sept. 4–7, 1990,* Plenary lecture; (g) P.L. Watson, *1st Int. Conf. f-Elements, Leuven, Belgium, Sept. 4–7, 1990,* Section lecture; (h) P.-F. Fu, L. Brard, C. Forsyth and T.J. Marks, submitted for publication; (i) P.-F. Fu, L. Brard and T.J. Marks, *Abstr. of Papers, 207th National Meet. American Chemistry Society, San Diego, CA, 1994,* INOR 40.

[5] (a) N. Koga and K. Morakuma, *J. Am. Chem. Soc., 115* (1993) 6883–6892; (b) S. Sakaki and M. Ieki, *J. Am. Chem. Soc., 115* (1993) 2373–2381; (c) *113* (1991) 5063–5065; (d) J.F. Harrod, T. Ziegler and V. Tschinke, *Organometallics, 9* (1990) 897–902; (e) T. Ziegler, V. Tschinke, L. Versluis, E.J. Baerends and W. Ravenek, *Bonding Energetics in Organometallic Compounds, ACS Symposium Series,* American Chemical Society, Washington, DC, 1990, pp. 1625–1637.

[6] (a) C.D. Hoff, *Prog. Inorg. Chem., 40* (1992) 503–561; (b) J.A. Martinho Simoes (ed.), *Energetics of Organometallic Species,* Kluwer, Dordrecht, Netherlands, 1992; (c) T.J. Marks (ed.), *Bonding Energetics in Organometallic Compounds, ACS Symposium Series,* American Chemical Society, Washington, DC, 1990; (d) J.A. Martinho Simoes and J.L. Beachamp, *Chem. Rev., 90* (1990) 629–688; (e) T.J. Marks (ed.), *Metal–Ligand Bonding Energetics in Organometallic Compounds, Polyhedron, 7* (1988).

[7] (a) H.A. Skinner and J.A. Connor, in J.F. Liebman and A. Greenberg (eds.), *Molecular Structure and Energetics,* Vol. 2, VCH, New York, 1987, Ch. 6; (b) H.A. Skinner and J.A. Connor, *Pure Appl. Chem., 57* (1985) 79–88; (c) R.G. Pearson, *Chem. Rev., 85* (1985) 41–59; (d) J.V. Mondal and D.M. Blake, *Coord. Chem. Rev., 47* (1983) 204–238; (e) M. Mansson, *Pure Appl. Chem., 55* (1983) 417–426.

[8] S.P. Nolan, M. Porchia and T.J. Marks, *Organometallics, 10* (1991) 1450–1457.

[9] B.K. Campion, J. Falk and T.D. Tilley, *J. Am. Chem. Soc., 109* (1987) 2049–2056.

[10] T.D. Tilley, *Organometallics, 4* (1985) 1452–1457.

[11] N.S. Radu and T.D. Tilley, *J. Am. Chem. Soc., 114* (1992) 8293–8295.

[12] G. Gutekunst and A.G. Brook, *J. Organomet. Chem., 225* (1982) 1–3.

[13] L.T. Reynolds and G. Wilkinson, *J. Inorg. Nucl. Chem., 2* (1956) 246–253.

[14] (a) S.P. Nolan, D. Stern and T.J. Marks, *J. Am. Chem. Soc., 111* (1989) 7844–7853; (b) L.E. Schock and T.J. Marks, *J. Am. Chem. Soc., 110* (1988) 7701–7715.

[15] N.K. Sung, F.F. Hsu, C.C. Chang, G.R. Her and C.T. Chang, *Inorg. Chem., 20* (1981) 2727–2728.

[16] H. Burger, W. Kilian and K. Burczyk, *J. Organomet. Chem., 21* (1970) 291–301.

[17] (a) D. Griller, J.J. Kanabus-Kaminska and A. Maccoll, *J. Mol. Struct., 163* (1988) 125–131; (b) R.C. Weast (ed.), *Handbook of Chemistry and Physics,* CRC, Boca Raton, FL, 65th edn., 1984, pp. F171–F190, and refs. therein; (c) S.W. Benson, *Thermochemical Kinetics,* Wiley, New York, 2nd edn., 1984, p. 309; (d) J.E. Huhee, *Inorganic Chemistry. Principles of Structure and Reactivity,* Harper and Row, New York, 3rd edn., 1983, A-28–A-40.

[18] L.E. Schock, A.M. Seyam and T.J. Marks, in Ref. [2b], pp. 1517–1530.

[19] (a) J.M. Kanabus-Kaminska, J.A. Hawari and D. Griller, *J. Am. Chem. Soc., 109* (1987) 5267–5268; (b) C. Chatgilialogu, A. Guerrini and Lucarini, *J. Org. Chem., 57* (1992) 3405–3409.

[20] (a) L. Ding and P. Marshall, *J. Am. Chem. Soc., 114* (1992) 5754–5758; (b) A. Goumri, W.-J. Yuan and P. Marshall, *J. Am. Chem. Soc., 115* (1993) 2539–2540.

[21] (a) W.J. Bullock, R. Walsh and K.D. King, *J. Phys. Chem., 98* (1994) 2595–2601; (b) R. Walsh, in Ref. [1], pp. 371–391; (c) A.R. Dias, H.P. Diogo, D. Griller, M.E. Minas de Piedade and J.A. Martinho-Simoes, in Ref. [6d], pp. 205–217. ($D(Ph_3Si\text{–}H) = 84.2(5)$ kcal mol$^{-1}$).

[22] P.M. Druce, B.M. Kinston, M.F. Lappert, T.R. Spalding and R.C. Srivastava, *J. Chem. Soc. A,* (1969) 2106–2110.

[23] H.R. Diogo, J. de Alencar Simoni, M.E. Minas de Piedade, A.R. Dias and J.A. Martinho-Simoes, *J. Am. Chem. Soc., 115* (1993) 2764–2774.

[24] (a) D.F. McMillen and D.M. Golden, *Ann. Rev. Phys. Chem., 33* (1982) 493–532; (b) J.A. Dean, *Handbook of Organic Chemistry,* McGraw-Hill, New York, 1987, pp. 3-19–3-27; (c) C.A. Carey and R.J. Sundberg, *Advanced Organic Chemistry, Part A: Structure and Mechanisms,* Plenum, 2nd edn., New York, 1984, pp. 11–17.

[25] A. Holt, W.P. Jarvie and J.J. Mallabar, *J. Organomet. Chem., 59* (1973) 141–144.

[26] M.E. Lee, M.A. North and P.P. Gaspar, *Phosphorus, Sulfur, Silicon Related Elements, 56* (1991) 203–212.

[27] X. Jemine, J. Goffart, J. Berthet and M. Ephritikhine, *J. Chem. Soc., Dalton Trans.,* (1992) 2439–2440.

[28] M.A. Giardello, W.A. King, S.P. Nolan, M. Porchia, C. Sishta and T.J. Marks, in J.A. Martinho Simoes (ed.), *Energetics of Organometallic Species,* Kluwer, Amsterdam, 1992, pp. 35–51.

[29] J.E. Huhee, *Inorganic Chemistry. Principles of Structure and Reactivity,* Harper and Row, New York, 3rd edn., 1983, pp. 133–149.

[30] (a) G.M. Smith, J.D. Carpenter and T.J. Marks, *J. Am. Chem. Soc., 108* (1986) 6805–6807; (b) M.I. Page, in M.I. Page (ed.), *The Chemistry of Enzyme Action,* Elsevier, New York, 1984, pp. 1–54; (c) M.I. Page, W.F. Jencks, *Proc. Natl. Acad. Sci. U.S.A., 68* (1971) 1678–1683.

[31] (a) D.H. Berry and Q. Jiang, *J. Am. Chem. Soc., 111* (1989) 8049–8051; (b) D.H. Berry, T.M. Koloski and P.J. Carroll, *Organometallics, 9* (1990) 2952–2962; (c) D.H. Berry, personal communication.

[32] G. Pilcher and H.A. Skinner, in F.R. Hartley and S. Patai, (eds.), *The Chemistry of the Metal–Carbon Bond,* Wiley, New York, 1982, pp. 43–90.

[33] (a) M. Brookhart and B.E. Grant, *J. Am. Chem. Soc., 115* (1993) 2151–2156, and refs. therein; (b) I. Ojima in S. Patai and Z. Rappoport (eds.), *The Chemistry of Organic Silicon Compounds,* Wiley, Chichester, UK, 1989, Ch. 25.

[34] H.Q. Liu and J.F. Harrod, *Organometallics, 11* (1992) 822–827, and refs. therein.

[35] (a) D.A. Armitage, in G. Wilkinson, F.G.A. Stone and E.W. Abel (eds.), *Comprehensive Organometallic Chemistry,* Pergamon, Oxford, 1982, Ch. 9.1; (b) L. Birkofer and O. Stuhl, in S. Patai

and Z. Rappoport (eds.), *The Chemistry of Organic Silicon Compounds,* Wiley, Chichester, UK, 1989, Ch. 10.

[36] (a) G. Jeske, H. Lauke, H. Mauermann, P.N. Swepston, H. Schumann and T.J. Marks, *J. Am. Chem. Soc., 107* (1985) 8091–8103; (b) P.L. Watson and G.W. Parshall, *Acc. Chem. Res., 18* (1985) 51–55; (c) Z. Lin and T.J. Marks, *J. Am. Chem. Soc., 109* (1987), 7979–7985; (d) B.J. Burger, M.E. Thompson, D.W. Cotter and J.E. Bercaw, *J. Am. Chem. Soc., 112* (1990), 1566–1577; (e) X. Yang, C.L. Stern, T.J. Marks, *Angew. Chem., Int. Ed. Engl., 31* (1992) 1375–1377.

[37] (a) G. Jeske, H. Lauke, H. Mauermann, H. Schumann and T.J. Marks, *J. Am. Chem. Soc., 107* (1985) 8111–8118; (b) C.M. Fendrick, L.D. Schertz, V.W. Day and T.J. Marks, *Organometallics, 7* (1988), 1828–1838; (c) G.A. Molander and J.O. Hoberg, *J. Org. Chem., 57* (1992) 3266–3268; (d) M.A. Giardello, V.P. Conticello, L. Brard, M.R. Gagné and T.J. Marks, *J. Am. Chem. Soc., 116* (1994) 10241–10254.

[38] Z. Lin and T.J. Marks, *J. Am. Chem. Soc., 112* (1990) 5515–5525.

[39] D.A. Armitage, in G. Wilkinson, F.G.A. Stone and E.W. Abel (eds.), *Comprehensive Organometallic Chemistry,* Pergamon, Oxford, 1982, Ch. 9.1, pp. 109–113.